

# How accurate is Limber's equation?

P. Simon

Institute for Astronomy, University of Edinburgh, Royal Observatory, Blackford Hill, Edinburgh EH9-3HJ, UK

e-mail: [psimon@roe.ac.uk](mailto:psimon@roe.ac.uk)

Argelander-Institut für Astronomie\*, Universität Bonn, Auf dem Hügel 71, 53121 Bonn, Germany

Received/Accepted

## ABSTRACT

**Aims.** The so-called Limber equation is widely used in the literature to relate the projected angular clustering of galaxies to the spatial clustering of galaxies in an approximate way. This note gives estimates of where the regime of applicability of Limber's equation stops.

**Methods.** This paper revisits Limber's equation, summarises its underlying assumptions, and compares its predictions to the accurate integral of which the Limber equation is an approximation for some realistic situations. Thereby, the accuracy of the approximation is quantified. Different cases of spatial correlation functions are considered.

**Results.** Limber's equation is accurate for small galaxy separations but breaks down beyond a certain separation that depends mainly on the ratio  $\sigma/r_m$  and to some degree on the power-law index of spatial clustering;  $\sigma$  is the  $1\sigma$ -width of the galaxy distribution in *comoving distance*, and  $r_m$  the mean comoving distance. Limber's equation introduces a 10% systematic error that may be important at a scale of about a few degrees or in some cases, narrow galaxy distributions for example, even at arcmin scales. As rule-of-thumb, a 10% relative error is reached at  $\sim 260 \sigma/r_m$  arcmin for  $\gamma \sim 1.6$ , if the spatial clustering is a power-law  $\xi \propto r^{-\gamma}$ . More realistic  $\xi$  are discussed in the paper.

**Conclusions.** Limber's equation becomes increasingly inaccurate for larger angular separations. Ignoring this effect and blindly applying Limber's equation can possibly bias results for the inferred spatial correlation. It is suggested to use in cases of doubt, or maybe even in general, the exact equation that can easily be integrated numerically in the form given in the paper. This would actually eliminate all problems discussed in this paper.

**Key words.** galaxies - statistics : cosmology - large-scale structure of Universe : cosmology - theory

## 1. Introduction

If the distance of individual galaxies is not known, but only statistically for a sample of galaxies on the whole, one has to infer the real-space correlation from the observed angular correlation on the sky. This task has been performed many times since the early days of galaxy surveys as, for example, in the pioneering work of Totsuji & Kihara (1969), Groth & Peebles (1977) and Davis et al. (1977) based on the Lick galaxy survey. To relate the projected correlation function,  $\omega(\theta)$ , to the spatial, three-dimensional correlation function,  $\xi$ , many authors use an approximation that was introduced by Limber (1953). This approximation is nowadays referred to as Limber's equation.

It will be shown in Sect. 2.2 that Limber's approximation diverges when galaxies are closely distributed. That Limber's equation breaks down for narrow distributions is

no surprise, as it is assumed that the distributions do not vary considerably over the coherence length of the spatial correlation function. But how wide has a distribution to be? How much do we bias our estimate for the angular correlation by using Limber's equation, and is there an alternative? These questions are addressed by this paper.

Peebles (1980, p.199) argued that this break-down occurs at separations of roughly  $30^\circ$ , but made assumptions about galaxy surveys that do not meet the standards of many contemporary wide-field surveys. Due to the availability of spectroscopic or photometric redshifts quite narrowly binned distributions are often used in current studies.

This paper delineates the circumstances in which Limber's approximation is valid and gives an alternative for situations where it is not valid. Throughout this paper a flat universe will be assumed.

The exact equation for  $\omega$  is given in Sect. 2.1. The thereafter following Sect. 2.2 summarises Limber's approximation and investigates why it breaks down for peaked galaxy distributions or beyond a certain angular separa-

\* Founded by merging of the Institut für Astrophysik und Extraterrestrische Forschung, the Sternwarte, and the Radioastronomisches Institut der Universität Bonn.

tion. Alternative approximations for cases of narrow distributions of galaxies or for larger  $\theta$  are given inside the Sect. 2.3. By looking at different distributions with varying widths and means, the accuracy of the Limber approximation is assessed in Sect. 3. The paper finishes with conclusions in Sect. 4.

## 2. Relation between spatial and angular correlation function

### 2.1. Exact relation with only some restrictions

Consider two number density fields of galaxies,  $n_1(\mathbf{r})$  and  $n_2(\mathbf{r})$ , as a function of the position  $\mathbf{r}$  within the comoving frame. One defines the spatial clustering, or spatial correlation function,  $\xi(\Delta\chi)$  in terms of the average number of pairs of  $n_1$ - and  $n_2$ -galaxies that can be found when considering small volumes  $dV_{1/2}$  with a separation of  $\Delta\chi = |\mathbf{r}_1 - \mathbf{r}_2|$ :

$$\langle n_1(\mathbf{r}_1)n_2(\mathbf{r}_2) \rangle dV_1 dV_2 = \langle n_1 \rangle \langle n_2 \rangle [1 + \xi(\Delta\chi)] dV_1 dV_2 . \quad (1)$$

$\langle \cdot \rangle$  denotes the ensemble average. It is already assumed here that the random fields  $n_{1,2}$  are statistically homogeneous and isotropic so that  $\xi$  is a function of the distance  $\Delta\chi$  only. If we have  $n_1 = n_2$ , then  $\xi(\Delta\chi)$  is an auto-correlation function of a galaxy number density field.

Observing the galaxy density fields as projections on the sky,

$$\hat{n}_i(\boldsymbol{\theta}) = \int_0^\infty dr q_i(r) n_i(r\boldsymbol{\theta}, r) , \quad (2)$$

yields a different correlation function,  $\omega(\theta)$ , when pairs of galaxies,  $\hat{n}_1$  and  $\hat{n}_2$ , within solid angles  $d\Omega_{1/2}$  of angular separation  $\theta$  are considered:

$$\langle \hat{n}_1(\boldsymbol{\theta}_1) \hat{n}_2(\boldsymbol{\theta}_2) \rangle d\Omega_1 d\Omega_2 = \langle \hat{n}_1 \rangle \langle \hat{n}_2 \rangle [1 + \omega(\theta)] d\Omega_1 d\Omega_2 . \quad (3)$$

Here,  $q_i(r)$  is a filter or weight function (of the number density) solely depending on the comoving radial distance  $r$ . In the context of galaxy number densities, this filter needs to be normalised to one, i.e.

$$\int_0^\infty dr q_i(r) = 1 ; \quad (4)$$

it specifies the frequency of galaxies within the distance interval  $[r, r + dr]$ . The details of the filter depend on the selection function of the survey. The vector  $\boldsymbol{\theta}$  is the direction of the line-of-sight. The observer is sitting at the origin of the reference frame,  $\mathbf{r} = 0$ , while other points on the line-of-sight are parametrised by  $r\boldsymbol{\theta}$ . To take into account a possible time-evolution of  $n_i$  the second argument in  $n_i(r\boldsymbol{\theta}, r)$  is supposed to parametrise the look-back time,  $t(r)$ , as a function of the comoving radial distance at which the random field is observed:

$$t(r) = \frac{1}{c} \int_0^r dr' a(r') , \quad (5)$$

where  $a(r)$  is the scale factor at comoving distance  $r$ , and  $c$  the vacuum speed of light.

As already mentioned the arguments stated above assume a Euclidean geometry for the Universe. This is not a strong restriction, though, because any other fiducial cosmological model can be incorporated by redefining the filter  $q_i$  – by absorbing  $F(x)$  in the (relativistic) Limber equation of Peebles (1980) (Chapter III, Sect. 56) into  $q_i$  – which leaves the form of (2) effectively unchanged.

Let us now derive a relation between  $\omega$  and  $\xi$ . Imagine we observe the spatial fluctuations ( $\langle n_i \rangle(r)$  is the mean density at cosmic time  $t(r)$ ),

$$\delta_{1,2}(r\boldsymbol{\theta}, r) \equiv \frac{n_{1,2}(r\boldsymbol{\theta}, r)}{\langle n_{1,2} \rangle(r)} - 1 , \quad (6)$$

of the two random fields as projection on the sky towards the direction  $\boldsymbol{\theta}$ :

$$\hat{\delta}_{1,2}(\boldsymbol{\theta}) = \int_0^\infty dr p_{1,2}(r) \delta_{1,2}(r\boldsymbol{\theta}, r) . \quad (7)$$

Here,  $p_i$  are the filters of the spatial fluctuations,  $\delta_i$ , that correspond to  $q_i$  (the filter of the density fields):<sup>1</sup>

$$p_i(r) = q_i(r) \langle n_i \rangle(r) \left[ \int_0^\infty dr q_i(r) \langle n_i \rangle(r) \right]^{-1} . \quad (8)$$

This relation between  $q_i$  and  $p_i$  follows from the definition of the density contrast of the projected (number) density:

$$\hat{\delta}_i(\boldsymbol{\theta}) = \frac{\hat{n}_i(\boldsymbol{\theta})}{\langle \hat{n}_i \rangle} - 1 . \quad (9)$$

If the mean density is constant, both associated filters  $p_i$  and  $q_i$  will be identical.

According to the definition of  $\omega$  we have for sight-lines  $\boldsymbol{\vartheta}_1$  and  $\boldsymbol{\vartheta}_2$  spanning an angle  $\theta = \angle \boldsymbol{\vartheta}_1, \boldsymbol{\vartheta}_2$ :

$$\begin{aligned} \omega(\theta) &= \langle \hat{\delta}_1(\boldsymbol{\vartheta}_1) \hat{\delta}_2(\boldsymbol{\vartheta}_2) \rangle \\ &= \int_0^\infty dr_1 \int_0^\infty dr_2 p_1(r_1) p_2(r_2) \langle \delta_1(r_1 \boldsymbol{\vartheta}_1, r_1) \delta_2(r_2 \boldsymbol{\vartheta}_2, r_2) \rangle \\ &\approx \int_0^\infty dr_1 \int_0^\infty dr_2 p_1(r_1) p_2(r_2) \xi \left( R, \frac{r_1 + r_2}{2} \right) , \end{aligned} \quad (10)$$

where

$$R \equiv \sqrt{r_1^2 + r_2^2 - 2r_1 r_2 \cos \theta} . \quad (12)$$

As before the second argument of the spatial correlation,  $\xi(R, r)$ , parametrises the time,  $t(r)$ , at which the spatial correlation function is observed.

Two assumptions had to be made to arrive at (11): a) the random fields  $\delta_{1,2}$ , and hence also their projections,  $\hat{\delta}_{1,2}$ , are statistically isotropic and homogeneous, and b) the time-evolution of  $\xi$  is small within the region where the product  $p_1(r_1)p_2(r_2)$  is non-vanishing. Due to assumption a)  $\omega$  depends only on  $\theta$  and is independent of the directions  $\boldsymbol{\vartheta}_{1,2}$ . Owing to assumption b) we can approximate the spatial correlation of fluctuations at different cosmic times (radial distances)  $t(r_1)$  and  $t(r_2)$  by a representative  $\xi$  at time  $(r_1 + r_2)/2$ .

Note that Eq. (11) is, under the previously stated assumptions, valid even for large  $\theta$ .

<sup>1</sup> In this paper the focus will be on the angular clustering and hence normalised  $p_i$  are assumed, albeit all equations and the conclusions are also valid for other types of projections.

## 2.2. Limber's approximation and its breakdown

Limber (1953) introduced several approximations in order to simplify the integral Eq. (11). The details of this approximation are given in Appendix A. Here only the result is quoted:

$$\omega(\theta) = \int_0^\infty d\bar{r} p_1(\bar{r}) p_2(\bar{r}) \int_{-\infty}^{+\infty} d\Delta r \xi(R, \bar{r}) \quad (13)$$

$$R \equiv \sqrt{\bar{r}^2 \theta^2 + \Delta r^2}. \quad (14)$$

The useful Eq. (13) has frequently been used in the astronomy community because it allows one to find an analytical expression (Peebles 1980) for  $\omega$  in case of a power-law like

$$\xi(r) = \left(\frac{r}{r_0}\right)^{-\gamma}, \quad (15)$$

( $r_0$  is the clustering length) namely

$$\omega(\theta) = A_\omega \left(\frac{\theta}{1 \text{ RAD}}\right)^{1-\gamma}. \quad (16)$$

The angular clustering amplitude at  $\theta = 1 \text{ RAD}$  is

$$A_\omega = \sqrt{\pi} r_0^\gamma \frac{\Gamma(\gamma/2 - 1/2)}{\Gamma(\gamma/2)} \int_0^\infty d\bar{r} p_1(\bar{r}) p_2(\bar{r}) \bar{r}^{1-\gamma}. \quad (17)$$

It has been found that a power-law  $\xi$  is a fairly good description of the true spatial correlation function (e.g. Zehavi et al. 2002) of galaxies for scales below  $\sim 15 \text{ Mpc/h}$ , which makes Limber's equation quite practical. Typical values are  $\gamma \sim 1.8$  and  $r_0 \sim 5 h^{-1} \text{ Mpc}$ .

However, due to the integral,  $A_\omega$  diverges to infinity if the width of the distributions  $p_{1,2}$  approaches zero and as long as  $p_{1,2}$  remain overlapping; the latter is trivially true if we are considering auto-correlations,  $p_1 = p_2$ . To make this point, let us assume that  $p_{1,2}$  are top-hat functions with centre  $r_c$  and width  $2\Delta r$ :

$$p_{1,2}(r) = \frac{1}{2\Delta r} \times \begin{cases} 1 & \text{for } r \in [r_c - \Delta r, r_c + \Delta r] \\ 0 & \text{otherwise} \end{cases}. \quad (18)$$

It follows for  $A_\omega$ :

$$A_\omega \propto \frac{1}{4\Delta r^2} \int_{r_c - \Delta r}^{r_c + \Delta r} d\bar{r} \bar{r}^{1-\gamma} \approx \frac{1}{2\Delta r} r_c^{1-\gamma}. \quad (19)$$

The last step is valid for small  $\Delta r \ll r_c$ , which shows that  $A_\omega$  diverges for narrow distributions as  $\Delta r^{-1}$ . This small calculation implies that Limber's equation possibly overestimates the angular correlation  $\omega$  to some degree.

In the astronomical literature, Eq. (13) is also known in other forms involving the three-dimensional power spectrum (e.g. Kaiser 1998; Hamana et al. 2004). No matter the form of Limber's equation, it always suffers from the divergence previously discussed and from the inaccuracies that are going to be discussed in the following.

## 2.3. Thin-layer approximation

Approximation Eq. (13) fails if the weight functions become delta-like functions, i.e. for galaxies being located inside one layer at comoving distance  $r_c$ . To obtain the correct solution for

$$p_{1,2}(r) = \delta_D(r - r_{1,2,c}) \quad (20)$$

(where  $\delta_D(r)$  is the Dirac delta function) we simply have to go back to Eq. (11) and find:

$$\omega(\theta) = \xi \left( \sqrt{r_{1,c}^2 + r_{2,c}^2 - 2r_{1,c}r_{2,c} \cos \theta}, \frac{r_{1,c} + r_{2,c}}{2} \right). \quad (21)$$

For  $r_{1,c} = r_{2,c} \equiv r_c$ , i.e. for auto-correlations which are mainly considered in this paper, we obtain as quite simple and intuitive result

$$\omega(\theta) = \xi \left( r_c \sqrt{2} \sqrt{1 - \cos \theta}, r_c \right) \approx \xi(r_c \theta, r_c). \quad (22)$$

This means that for very narrow filter we essentially observe a rescaled  $\xi$ . An immediate consequence is that  $\omega$  has *the same slope*,  $\gamma$ , as  $\xi$ , if  $\xi$  happens to be a power-law as in Eq. (15); on the other hand for wide filter, in the regime where Limber's approximation is accurate,  $\omega$  has a shallower slope of  $\gamma - 1$ .

It can be shown, as done in Appendix B, that the thin-layer approximation is not just a sole particularity of extremely peaked weight functions  $p$ . The solution is asymptotically approached by (11) if the separation  $\theta$  gets large enough, namely  $\theta \gtrsim \sqrt{2} \frac{\sigma}{r_m}$  in the case of auto-correlations  $p(r) \equiv p_1(r) = p_2(r)$ ;  $\sigma$  is the  $1\sigma$ -width and  $r_m$  the mean of the weight  $p(r)$  (both in units of comoving distance).

This discussion shows that Limber's equation and the thin-layer equation are approximations for two extremes, namely for small  $\theta$  and large  $\theta$ , respectively. The transition point between the two regimes is mainly determined by the ratio  $\sigma/r_m$  implying that the accuracy of Limber's equation is, in the case of auto-correlations at least, mainly determined by this ratio.

## 2.4. Numerical integration of the exact equation

With the availability of computers there is no longer a need to use any approximations in this context. However, one finds that solving Eq. (11) (or A.2) by numerical integration with a power-law  $\xi$  is cumbersome because many fine bins are needed to achieve the desired accuracy. This is mainly due to the argument  $R$  in  $\xi$  which does not sample  $\xi$  on a log-scale, which however should be aimed at with a power-law like  $\xi$ . It is advisable to consider a numerical integration with different coordinates such that the spatial part of  $\xi$  depends just on one integration variable  $R$ .

This can be done by changing the integration variable in the inner integral of (A.2) from  $\Delta r$  to  $R$ :

$$\omega(\theta) = \frac{1}{1 + \cos \theta} \int_0^\infty d\bar{r} \int_{\bar{r} \sqrt{2(1 - \cos \theta)}}^{2\bar{r}} dR Q(\bar{r}, \Delta) \xi(R, \bar{r}) \frac{R}{\Delta}, \quad (23)$$

where

$$\Delta \equiv \frac{1}{\sqrt{2}} \sqrt{\frac{R^2 - 2\bar{r}^2(1 - \cos \theta)}{1 + \cos \theta}}, \quad (24)$$

and

$$Q(\bar{r}, \Delta) \equiv p_1(\bar{r} - \Delta)p_2(\bar{r} + \Delta) + p_1(\bar{r} + \Delta)p_2(\bar{r} - \Delta). \quad (25)$$

The expression (23) may look more complicated than (11) or (A.2) but is superior for numerical integrations: The integration over  $R$  can be done on a logarithmic scale, the integration limits for  $R$  can be adjusted for  $\xi$ 's that effectively vanish somewhere in the integration interval. Furthermore, also the integration limits for  $\bar{r}$  can be adjusted if  $Q(\bar{r}, \Delta)$  vanishes effectively somewhere within the integration limits.

### 3. Accuracy of Limber's equation

The aim of this section is to assess the accuracy of Limber's equation by comparing its predictions to the exact solution for the angular correlation function. For this purpose, different spatial clustering models  $\xi$  are used that are constant in time. Moreover, the focus is on auto-correlations  $\omega$ , hence  $p_1(r) = p_2(r) \equiv p(r)$ .

In order to quantify the accuracy of Limber's approximation, the exact solution Eq. (11) is solved by numerical integration, by means of (23), and compared to the result from Limber's equation (13). In order to make a fair comparison, the same small angle approximation as in (13) is applied to the exact equation, which as it is written in (23) does, of course, not require small galaxy separations:

$$\frac{1}{1 + \cos \theta} \approx \frac{1}{2}, \quad (26)$$

$$\Delta \approx \frac{1}{2} \sqrt{R^2 - \bar{r}^2 \theta^2}, \quad (27)$$

$$\bar{r} \sqrt{2(1 - \cos \theta)} \approx \bar{r} \theta. \quad (28)$$

#### 3.1. Model galaxy probability distribution

The intention is to study the accuracy of Limber's equation for relatively narrow distributions of galaxies,

$$p(r) \propto r^2 \exp\left(-\frac{1}{2} \frac{(r - r_c)^2}{\sigma_p^2}\right). \quad (29)$$

Thus, galaxies selected by this filter are centred on  $r_c$  with some scatter  $\sigma_p$ . The prefactor  $r^2$  accounts for the apparent increase in the angular galaxy number density with distance  $r$  within the light-cone which only for moderately wide or wide distributions becomes relevant. The prefactor has been added to make the distribution more realistic.

The parameter  $\sigma_p$  in (29) is not identical with the  $1\sigma$ -scatter of the distribution, and  $r_m$  is not identical with  $r_c$ ; this is only roughly correct for small  $x \equiv \sigma_p/r_c$ . However,

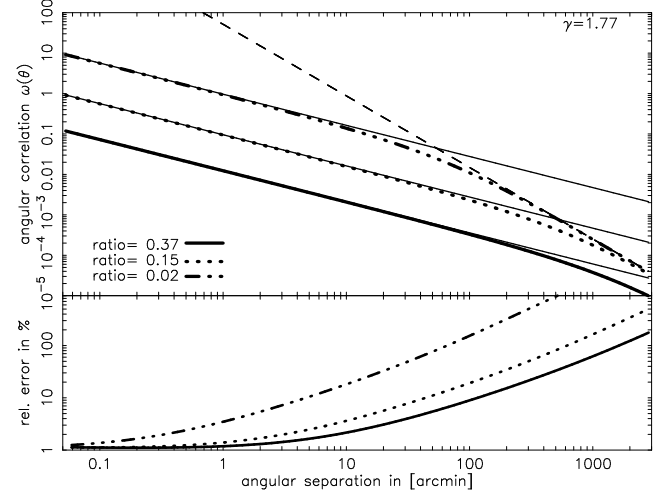


**Fig. 1.** Shown here is the angular correlation function  $\omega$  for three different ratios  $\frac{\sigma}{r_m}$  of the galaxy distribution, see Eq. (29),  $r_c = 2 h^{-1}$  Gpc. The spatial correlation,  $\xi$ , is a power-law with slope  $\gamma = 1.77$  and clustering amplitude  $r_0 = 5.4 h^{-1}$  Mpc as roughly found for real galaxies. The thick lines are the numerical integrations of the exact equation, Eq. (23), while the thin solid lines are the predictions by Limber's equation, Eq. (16). The small angle approximations assumed in Limber's equation are also applied to the exact equation. The relative difference between exact and Limber solution is plotted in the bottom small panel. The thin dashed line is the exact solution for an extremely peaked galaxy distribution, Eq. (22).

it can be shown that the ratio  $y \equiv \sigma/r_m$  is entirely a function of  $x$ , namely approximately

$$y \approx x \frac{\sqrt{3x^4 + 1}}{3x^2 + 1} [1 + 0.01x^2 - \exp(-1.29x^{-1.73})], \quad (30)$$

with an accuracy of a few percent for  $0 \leq x \lesssim 2.5$ . This relation is used in the following to find a  $p(r)$  for given  $y$  and  $r_c$ .

#### 3.2. Power-law spatial correlation functions

The angular clustering,  $\omega$ , for three different galaxy distributions has been computed for the Figure 1;  $\xi$  is the same in all three cases. As expected, Limber's equation describes the exact solution quite well for small angular separations  $\theta$  but starts to deviate from the  $\gamma - 1$  power-law for larger separations, becoming steeper and tending to look very much like the thin-layer solution (22) (thin dashed line) which has the slope  $\gamma$ . Therefore, the exact angular clustering is a broken power-law if the spatial clustering is a power-law. This behaviour is expected from the discussion in Appendix B.

The break position is important for the Limber approximation: The closer one gets to the break position (and the farther beyond it), the more inaccurate is Limber's description. When  $\xi$  can be assumed to be a power-law

we can define a sensible position  $\theta_{\text{break}}$  for the break by working out where the Limber and the thin-layer approximation intersect. As shown in Appendix C this is at:

$$\theta_{\text{break}} \approx \frac{2\sqrt{3}}{\sqrt{\pi}} \frac{\Gamma(\gamma/2)}{\Gamma(\gamma/2 - 1/2)} \frac{\sigma}{r_m}. \quad (31)$$

This relation reflects what has already been seen in the foregoing discussion. The break position is mainly determined by the ratio  $\sigma/r_m$  – but is also influenced by the slope  $\gamma$  of  $\xi$ : the prefactor of  $\sigma/r_m$  in (31) varies between 0.31 and 1.18 for  $\gamma = 1.2, 2.1$ , respectively: steeper  $\xi$  are projected more accurately by Limber’s equation than shallower  $\xi$ .

The relative error of Limber’s approximation at the break position is already large, roughly 100%. Therefore, the validity regime of this approximation stops well below the break position. As a rule-of-thumb, the relative error is about 10% at  $\theta_{\text{break}}/10$  which has been estimated from several plots like Figure 1. Therefore, a 10% error is reached at about  $\sim 260 \sigma/r_m$  arcmin for  $\gamma \sim 1.6$ .

### 3.3. More realistic galaxy clustering

Although (spatial) galaxy clustering is empirically well described by a power-law on scales below  $r \sim 15$  Mpc/h,  $\xi(r)$  on large cosmological scales eventually adopts the shape of the dark matter clustering which does not have a constant slope  $\gamma$  (e.g. Weinberg et al. 2004). Therefore, the previous discussion is only applicable if the effective physical scales, that correspond to the angular separation interval under investigation, are below  $r \sim 15$  Mpc/h. In the opposite case, we expect that the accuracy of Limber’s equation is not only a function of  $\sigma/r_m$  and an average of  $\gamma$ , but also a function of  $r_m$ .

To obtain more realistic  $\xi(r)$ , two representative models for galaxy clustering, based on a halo-model as in Magliocchetti & Porciani (NFW parameters; 2003), are used in this section: one  $\xi$  is supposed to represent the clustering of galaxies that preferentially inhabit dark matter haloes of larger mass ( $M_{\text{halo}} \geq 10^{12.6} M_{\text{sun}}$ ; “red galaxies”), another  $\xi$  describes galaxies that also live in smaller mass haloes ( $M_{\text{halo}} \geq 10^{11} M_{\text{sun}}$ ; “blue galaxies”). These two  $\xi$ ’s are placed at different redshifts between  $0 \leq z \leq 5$ , are “observed” on the sky through filters  $p(r)$  of varying widths  $\sigma/r_m$ , and compared to Limber’s equation in order to work out the relative error. As to the accuracy of Limber’s equation the amplitude of the correlation functions is irrelevant, it is only the shape that matters. For all redshifts considered the same  $\xi$  is assumed, that is the halo-model prediction for  $z = 0$ . To give an estimate of the relative error of narrow filters, this should be a fair assumption. See Figure 2 for a particular example of the angular clustering.

Figure 3. shows the estimated separation limits. The dependence of the filter on the centre,  $r_m$ , however can clearly be seen, becoming weaker for larger  $r_m$ . The difference between red and blue galaxies is most pronounced for small  $r_m$  but there are clear differences for  $\sigma/r_m \lesssim 0.02$ ,

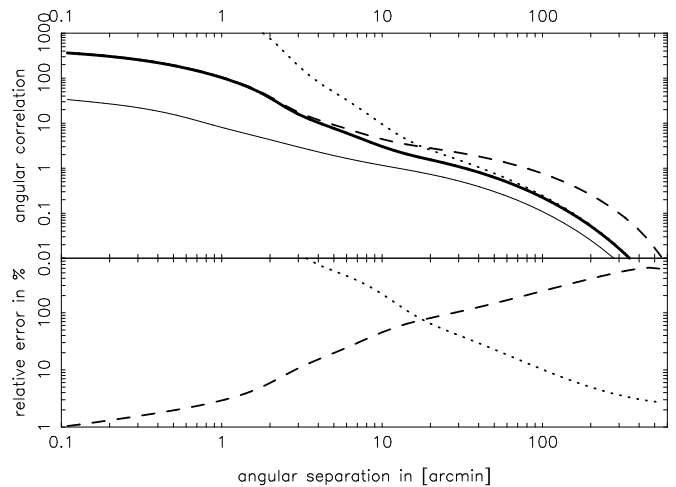


**Fig. 2.** Angular clustering (arbitrary scaling) of the red galaxy sample (upper panel, thick solid line) centred on  $z = 0.2$ , the relative width of the distribution in comoving distance is  $\sigma/r_m = 0.02$ . For comparison, also in the upper panel, the clustering of the blue population is plotted as well (thin solid line). The dashed and dotted line are the approximate solutions according to Limber’s equation and the thin-layer approximation (upper panel). The lower panel depicts the relative error of the Limber (dashed) and thin-layer solution (dotted) for the red galaxies, respectively.

even for large  $r_m$ . Limber’s prediction of the angular correlations of red galaxies is more accurate than the predictions for blue galaxies because on megaparsec-scales  $\xi$  of red galaxies is steeper than  $\xi$  of blue galaxies.

## 4. Summary and conclusions

The Limber equation is an approximate solution for the angular correlation function of objects, mainly applied in the context of galaxies, for a given spatial correlation function.

In this paper, it was shown that the assumptions made for Limber’s approximation become inaccurate beyond a certain angular separation, which essentially depends on  $\sigma/r_m$  and the shape of the spatial correlation function. It should be emphasised that this inaccuracy has no relation to the flat-sky approximation (small separations) that is commonly adopted when working with Limber’s equation.

Beyond what separation  $\theta$  does Limber’s approximation become wrong by 10%? For power-law  $\xi$ ’s this separation depends entirely on  $\gamma$  and  $\sigma/r_m$  of the filter (selection function) used. Spatial correlations with larger  $\gamma$  are treated more accurately by Limber’s equation than  $\xi$  with shallower  $\gamma$ . As a rule-of-thumb, a systematic error of 10% is reached at about  $260 \frac{\sigma}{r_m}$  arcmin for  $\gamma \sim 1.6$ .

For more realistic  $\xi$ ’s with a running slope  $\gamma$ , the separation is also dependent on  $r_m$ , the centre of the filter. Even for relatively wide filters with  $\sigma/r_m \sim 0.2$ , Limber’s equation becomes inaccurate on the 10% level at a scale of

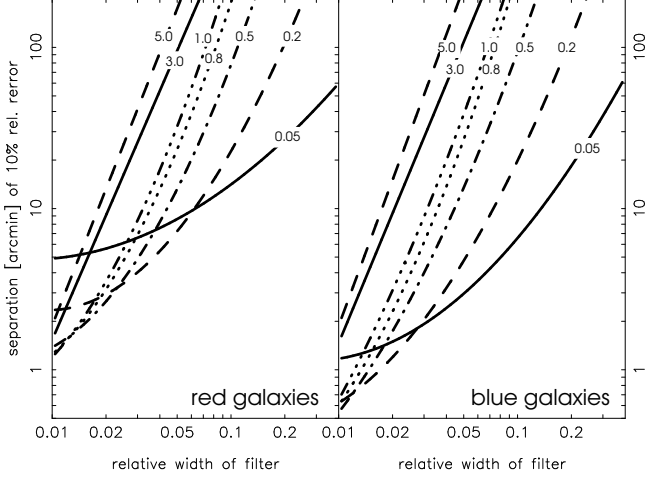


**Fig. 3.** Galaxy separation, as a function of  $\sigma/r_m$  of the filter, at which Limber’s equation becomes inaccurate by 10% for red (left panel) and blue (right panel) galaxies. Different lines correspond to different  $r_m$ ; the corresponding redshifts are the line labels. Note that for estimating the relative error the *local* correlation function of red and blue galaxies was simply moved to higher redshifts. The (flat) fiducial cosmology assumes  $\Omega_m = 0.3$ .

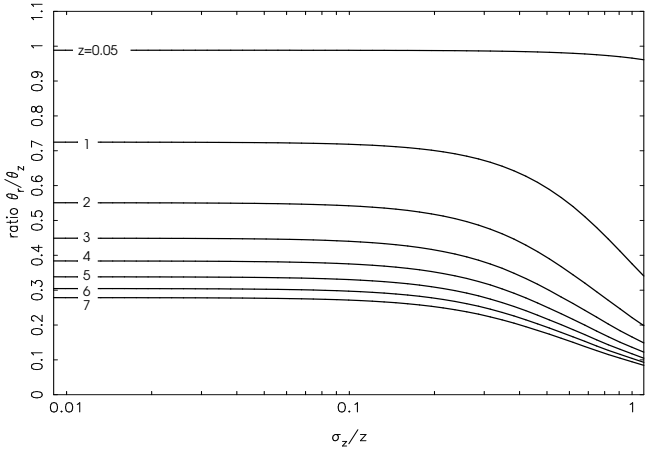


**Fig. 4.** Filter (galaxy distributions)  $p(r)$  appear “wider” in redshift,  $p_z(z) = p(r(z)) \frac{dr}{dz}$ , than in comoving distance, i.e. usually  $(\theta_z \equiv \sigma_z/\bar{z}) \geq (\theta_r \equiv \sigma_r/r_m)$  where  $\sigma_z$  and  $\sigma_r$  are the  $1\sigma$ -widths in redshift, and comoving distance, respectively;  $r_m$  is the mean of the weight in comoving distance, while  $\bar{z}$  is the mean in redshift. To give an estimate of the correction  $\theta_r/\theta_z$  ( $y$ -axis) as function of  $\theta_z$  ( $x$ -axis)  $p_z$ ’s are assumed that are close to Gaussians. Each solid line corresponds to different means  $\bar{z} \in [0.05, 7]$  (upper to lower line).

a few degrees separation. On the other hand, for narrow filters of about  $\sigma/r_m \lesssim 0.02$ , a systematic error of 10% is already reached after  $\sim 10'$  (or even a few arcmin depending on  $r_m$ ).

galaxy sample	$\bar{z} \pm \sigma_z$	$\sigma/r_m$
<b>Quadri et al. (2007)</b>		
<i>K</i> -dropouts	$z = 2 \dots 3.5$	$\sim 0.16$
<b>Lee et al. (2006)</b>		
<i>U</i> -dropouts	$3.2 \pm 0.3$	$\sim 0.04$
<i>B</i> <sub>435</sub> -dropouts	$3.8 \pm 0.3$	$\sim 0.03$
<i>V</i> <sub>606</sub> -dropouts	$4.0 \pm 0.3$	$\sim 0.02$
<b>Overzier et al. (2006)</b>		
<i>i</i> <sub>775</sub> -dropout	$6.0 \pm 0.5$	$\sim 0.03$
<b>Adelberger et al. (2005)</b>		
BM	$1.69 \pm 0.30$	$\sim 0.12$
BX	$2.24 \pm 0.37$	$\sim 0.09$
LBGs	$2.94 \pm 0.30$	$\sim 0.05$
<b>Hildebrandt et al. (2005)</b>		
LBGs	$2.96 \pm 0.24$	$\sim 0.04$
<b>Ouchi et al. (2004)</b>		
<i>BRi</i> – LBGs	$4.0 \pm 0.5$	$\sim 0.05$
<i>Vi</i> <i>z</i> – LBGs	$4.7 \pm 0.5$	$\sim 0.04$
<i>Ri</i> <i>z</i> – LBGs	$4.9 \pm 0.3$	$\sim 0.02$
LAE	$4.86 \pm 0.03$	$\sim 0.003$

**Table 1.** List of typical values for the relative width of the survey selection function,  $\sigma/r_m$  (comoving distance), in recent works using the dropout technique (LBGs: Lyman-break galaxies, LAE: Ly $\alpha$ -emitter). Note that typically only separations less than about one arcmin are considered so that the accuracy of Limber’s equation is, apart from the only LAE study in the list, no real issue.

Note that a filter can appear quite wide, i.e.  $\sigma_z/\bar{z}$  is large, as a function of redshift  $z$  while it is actually quite narrow as a function of comoving distance, the latter being the relevant parameter for the accuracy of Limber’s equation. In particular, this means that applying Limber’s equation to high redshift galaxies may be a problem. The reader might find Figure 4 useful to quickly look up the approximate conversion between  $\sigma_z/\bar{z}$  and  $\sigma_r/r_m$ .

Table 1 shows a small list of some recent studies of the high-redshift universe using the dropout-technique. According to the table the relative width of the selection filter frequently reaches values near 0.03. Therefore, Limber’s equation should in these and similar studies not be used when separations larger than  $\sim 20'$  are considered.

In cases where Limber’s approximation is in doubt, that one uses the exact Eq. (23) that can easily be integrated numerically.

Limber’s approximation is also used in gravitational lensing to quantify correlations between the gravity-induced distortions of faint galaxy images (see e.g. Bartelmann & Schneider 2001; Kaiser 1998). In this case, the filter function relevant for lensing is the lensing efficiency that, quite naturally, has a wide distribution; one can roughly estimate  $\sigma/r_m \approx 0.22$  if the source galaxies have a typical value of  $z_s = 1$ . The centre of this filter is at about  $\bar{z} \approx 0.5$ . These values will depend on the distribution of source galaxies in redshift and the fiducial cosmological model. Taking these values as a rough estimate of the relative lensing filter width and centre, and assum-

ing that the dark matter clustering is somewhere between the clustering of red and blue galaxies, one can infer from Figure 3 that a two-point *auto-correlation* function of the convergence, based on Limber's equation, is accurate to about 10% for separations less than several degrees; beyond that, an alternative description should be used.

*Acknowledgements.* I would like to thank Hendrik Hildebrandt and, in particular, Peter Schneider for carefully reading the manuscript, and their comments. This work was supported by the Deutsche Forschungsgemeinschaft (DFG) under the project SCHN 342/6-1. Furthermore, I am grateful for the kind hospitality of the Karolinska Institute, Stockholm, and David Kitz Krämer.

## References

- Adelberger, K. L., Steidel, C. C., Pettini, M., et al. 2005, *ApJ*, 619, 697
- Bartelmann, M. & Schneider, P. 2001, *Physics Reports*, 340, 291
- Davis, M., Groth, E. J., & Peebles, P. J. E. 1977, *ApJ*, 212, L107
- Groth, E. J. & Peebles, P. J. E. 1977, *ApJ*, 217, 385
- Hamana, T., Ouchi, M., Shimasaku, K., Kayo, I., & Suto, Y. 2004, *MNRAS*, 347, 813
- Hildebrandt, H., Bomans, D. J., Erben, T., et al. 2005, *A&A*, 441, 905
- Kaiser, N. 1998, *ApJ*, 498, 26
- Lee, K.-S., Giavalisco, M., Gnedin, O. Y., et al. 2006, *ApJ*, 642, 63
- Limber, D. N. 1953, *ApJ*, 117, 134
- Magliocchetti, M. & Porciani, C. 2003, *MNRAS*, 346, 186
- Ouchi, M., Shimasaku, K., Okamura, S., et al. 2004, *ApJ*, 611, 685
- Overzier, R. A., Bouwens, R. J., Illingworth, G. D., & Franx, M. 2006, *ApJ*, 648, L5
- Peebles, P. J. E. 1980, *The large-scale structure of the universe* (Research supported by the National Science Foundation. Princeton, N.J., Princeton University Press, 1980. 435 p.)
- Quadri, R., van Dokkum, P., Gawiser, E., et al. 2007, *ApJ*, 654, 138
- Totsuji, H. & Kihara, T. 1969, *PASJ*, 21, 221
- Weinberg, D. H., Davé, R., Katz, N., & Hernquist, L. 2004, *ApJ*, 601, 1
- Zehavi, I., Blanton, M. R., Frieman, J. A., et al. 2002, *ApJ*, 571, 172

## Appendix A: Details of Limber's approximation

In order to find an approximation of Eq. (11), one introduces for convenience new coordinates,

$$\bar{r} \equiv \frac{r_1 + r_2}{2} ; \quad \Delta r \equiv r_2 - r_1 , \quad (\text{A.1})$$

which are the mean radial comoving distance and difference of radial distances, respectively, of a pair of galaxies.

This change of coordinates renders (11) in the following manner:

$$\omega(\theta) = \int_0^\infty d\bar{r} \int_{-2\bar{r}}^{+2\bar{r}} d\Delta r p_1\left(\bar{r} - \frac{\Delta r}{2}\right) p_2\left(\bar{r} + \frac{\Delta r}{2}\right) \xi(R', \bar{r}) \quad (\text{A.2})$$

where

$$R' \equiv \sqrt{2\bar{r}^2(1 - \cos \theta) + \frac{\Delta r^2}{2}(1 + \cos \theta)} . \quad (\text{A.3})$$

This equation is simplified further by making the following approximations which are roughly satisfied for wide weight functions  $p_{1,2}$ , and for  $\xi$  that fall off sufficiently fast over the typical width of  $p_{1,2}$ :

$$p_1\left(\bar{r} - \frac{\Delta r}{2}\right) p_2\left(\bar{r} + \frac{\Delta r}{2}\right) \approx p_1(\bar{r}) p_2(\bar{r}) , \quad (\text{A.4})$$

$$\int_{-2\bar{r}}^{+2\bar{r}} d\Delta r \xi(R', \bar{r}) \approx \int_{-\infty}^{+\infty} d\Delta r \xi(R', \bar{r}) . \quad (\text{A.5})$$

Especially the approximation (A.4) is characteristic for Limber's equation. It is justified if the weight functions  $p_{1,2}$  do not “vary appreciably” (Bartelmann & Schneider 2001, p.43) over the coherence length of structures described by  $\xi$  – typically a few hundred Mpc in the context of cosmological large-scale structure –, which means we consider cases in which the coherence length is small compared to the width of the weight functions  $p_{1,2}$ . In total, these assumptions lead to the (relativistic) Limber equation (Limber 1953; Peebles 1980):

$$\omega(\theta) = \int_0^\infty d\bar{r} p_1(\bar{r}) p_2(\bar{r}) \int_{-\infty}^{+\infty} d\Delta r \xi(R, \bar{r}) , \quad (\text{A.6})$$

where

$$R \equiv \sqrt{\bar{r}^2 \theta^2 + \Delta r^2} . \quad (\text{A.7})$$

For historical reasons, as a further approximation it is assumed in the above equations that we are dealing with small angles of separation,  $\theta$ , by which we can introduce:

$$1 + \cos \theta \approx 2 ; \quad 1 - \cos \theta \approx \frac{\theta^2}{2} . \quad (\text{A.8})$$

These two approximations are accurate to about 10% for angles smaller than  $\theta \lesssim 40^\circ$  which covers the typical range of investigated separations. Usually, when employing Limber's equation this approximation is automatically used.

## Appendix B: Approximation for larger separations

It will be shown here that the thin-layer solution of the Sect. 2.3 is in fact asymptotically approached if the separation  $\theta$  only gets large enough.

To see why the exact solution behaves like this we have to go back to Eq. (A.2) and in particular (A.3). From that we can work out what happens for larger  $\theta$ . Note that

the following focuses on auto-correlations. The  $\Delta r$ -term in (A.3) can be neglected compared to the  $\bar{r}$ -term if

$$2\bar{r}^2(1 - \cos \theta) \gg \frac{\Delta r^2}{2}(1 + \cos \theta) \quad (\text{B.1})$$

$$\iff \frac{\Delta r}{2\bar{r}} \tan^{-1} \left( \frac{\theta}{2} \right) \ll 1. \quad (\text{B.2})$$

Let us say the distribution  $p$  of galaxies has a characteristic width (variance) of  $\sigma$  and a mean of  $r_m$ . Pairs of galaxies from this distribution will typically have  $\bar{r} = \langle (r_1 + r_2)/2 \rangle \approx r_m$  and for their mutual distance  $\Delta r \approx \sqrt{\langle (r_1 - r_2)^2 \rangle} \approx \sqrt{2}\sigma$ . Therefore, the condition (B.2) will be given for  $\theta$  large enough to fulfil

$$\tan \left( \frac{\theta}{2} \right) \gg \frac{\sigma}{\sqrt{2}r_m}, \quad (\text{B.3})$$

or for small  $\theta$  (10% accuracy for  $\theta \lesssim 60^\circ$ ) approximately

$$\theta \gg \sqrt{2} \frac{\sigma}{r_m}. \quad (\text{B.4})$$

In this regime, where the  $\Delta r$ -term in  $R'$  is negligible, Eq. (A.2) simplifies to

$$\omega(\theta) = \int_0^{+\infty} d\bar{r} F(\bar{r}) \xi \left( \bar{r} \sqrt{2} \sqrt{1 - \cos \theta}, \bar{r} \right), \quad (\text{B.5})$$

which is a family of thin-layer solutions (22) weighted averaged with the kernel

$$F(\bar{r}) \equiv \int_{-2\bar{r}}^{+2\bar{r}} d\Delta r p \left( \bar{r} + \frac{\Delta r}{2} \right) p \left( \bar{r} - \frac{\Delta r}{2} \right). \quad (\text{B.6})$$

Already for moderately wide  $p(r)$ ,  $F(r)$  is relatively peaked, so that for large enough  $\theta$ , Eq. (B.5) is close to the solution (22) with  $r_c \approx r_m$ . Note that  $F(r)$  is normalised to one.

## Appendix C: Break position

Limber's equation is an accurate description for small  $\theta$  and the ‘‘thin-layer’’ solution, Eq. (22), is an approximate solution for larger  $\theta$ . For power-law like spatial correlation functions,  $\xi \propto r^{-\gamma}$ , a sensible definition for the position of the break is at the angle  $\theta_{\text{break}}$  (in RAD) where both approximations intersect:

$$A_\omega \theta_{\text{break}}^{1-\gamma} = \xi(\sqrt{2}\sqrt{1 - \cos \theta_{\text{break}}} r_m). \quad (\text{C.1})$$

Using (15) and (17) one obtains after some algebra:

$$\theta_{\text{break}}^{1-\gamma} \left( \sqrt{2}\sqrt{1 - \cos \theta_{\text{break}}} \right)^\gamma = \frac{\Gamma(\gamma/2)}{\sqrt{\pi} \Gamma(\gamma/2 - 1/2)} \left[ r_m^\gamma \int_0^\infty d\bar{r} p^2(\bar{r}) \bar{r}^{1-\gamma} \right]^{-1}. \quad (\text{C.2})$$

For  $\gamma \in [1, 2]$  the left-hand side of the previous equation is for  $\theta_{\text{break}} \lesssim 60^\circ$  within 10% accuracy just

$$\theta_{\text{break}}^{1-\gamma} \left( \sqrt{2}\sqrt{1 - \cos \theta_{\text{break}}} \right)^\gamma \approx \theta_{\text{break}}. \quad (\text{C.3})$$

Thus, this is a reasonable approximation to use.

The relation (C.2) is useful because it allows one to estimate the expected position of the break in the power-law behaviour of  $\omega$ . As the accuracy of Limber's equation is primarily an issue for narrow  $p$  we can derive from (C.2) a rule-of-thumb for the break position. For narrow  $p$ , it is sensible to assume a top-hat function as in Eq. (18). Then, employing (19), (C.3) and (C.2) one gets:

$$\theta_{\text{break}} = \frac{2\sqrt{3}}{\sqrt{\pi}} \frac{\Gamma(\gamma/2)}{\Gamma(\gamma/2 - 1/2)} \frac{\sigma}{r_m}. \quad (\text{C.4})$$

Note that the variance of the top-hat is  $\sigma = \Delta r/\sqrt{3}$ , where  $\Delta r$  is the width of the top-hat.